ISSN 1027-5495. Functional Materials, 27, No.3 (2020), p. 559-566.
doi:https://doi.org/10.15407/fm27.03.559

Surface polaritons in optical-anisotropic $Mg_XZn_{1-X}O$/6H–SiC structures

***O.V.Melnichuk*[1], *L.Yu.Melnichuk*[1], *N.O.Korsunska*[2], *L.Yu.Khomenkova*[2,3], *Ye.F.Venger*[2]**

[1]M. Gogol State University of Nizhyn, 2 Hrafska Str., 16600 Nizhyn, Ukraine
[2]V.Lashkaryov Institute of Semiconductor Physics, National Academy of Sciences of Ukraine, 41 Pr. Nauky, 03650 Kyiv, Ukraine
[3]National University "Kyiv-Mohyla Academy", 2 Skovorody Str., 04070 Kyiv, Ukraine

Received January 8, 2020

Theoretical modeling of the excitation and propagation of surface phonon (plasmon-phonon) polaritons in $Mg_XZn_{1-X}O$/6H–SiC structure was performed using a multi-oscillator model, which takes into account the additive contribution of the phonon and plasmon-phonon subsystem parameters to the dielectric permittivity of the material. The simulation was carried out for both $Mg_XZn_{1-X}O$ films and 6H–SiC substrates with different free carrier concentrations. It was determined the frequency windows where surface polaritons of different types can be excited. The dispersion dependences for $Mg_XZn_{1-X}O$/6H–SiC structure were obtained taking into account the interaction of the phonon and plasmon-phonon subsystems of the film and the substrate. A three-dimensional representation of reflection coefficient of this structure was constructed.

Keywords: surface polaritons, attenuated total reflection, dielectric constant, magnesium-zinc oxide, silicon carbide, dispersion law.

Поверхневі поляритони в оптично-анізотропних структурах $Mg_XZn_{1-X}O$/6H–SiC.
О.В.Мельничук, Л.Ю.Мельничук, Н.О.Корсунська, Л.Ю.Хоменкова, Є.Ф.Венгер

Теоретично досліджено можливість збудження та розповсюдження поверхневих фононних (плазмон-фононних) поляритонів у структурі $Mg_XZn_{1-X}O$/6H–SiC. Використано модель з багатьма осциляторами, яка враховує адитивний вклад параметрів фононної та плазмон-фононної підсистем у діелектричну проникність матеріалу. Розрахунки проведено як для плівок $Mg_XZn_{1-X}O$, так і для підкладок 6H–SiC з різною концентрацією вільних носіїв. Виявлено частотні вікна, в яких можуть збуджуватися поверхневі поляритони різного типу. Одержано дисперсійні залежності для вказаної структури за врахування взаємодії фононної та плазмон-фононної підсистем плівки та підкладки, побудовано поверхню порушеного повного внутрішнього відбивання, яка являє собою тривимірне подання коефіцієнта відбивання зазначеної вище структури.

Теоретически исследована возможность возбуждения и распространения поверхностных фононных (плазмон-фононных) поляритонов в структуре $Mg_XZn_{1-X}O$/6H–SiC. Использована многоосцилляторная модель, которая учитывает аддитивный вклад параметров фононной и плазмон-фононной подсистем в диэлектрическую проницаемость материала. Расчеты проведены как для пленок $Mg_XZn_{1-X}O$, так и для подложек 6H–SiC с разной концентрацией свободных носителей. Выявлены частотные окна, в которых могут возбуждаться поверхностные поляритоны различного типа. Получены дисперсионные зависимости для указанной структуры с учетом взаимодействия фононной и плазмон-фононной подсистем пленки и подложки, построена поверхность нарушенного полного внутреннего отражения, которая представляет собой трехмерное представление коэффициента отражения структуры $Mg_XZn_{1-X}O$/6H–SiC.

1. Introduction

Recent achievements in the field of nano- and optoelectronics brought the demand for the elaboration of non-destructive approaches for the characterization of different semiconductor and dielectric materials and structures on their basis. Such approaches become important for the determination of the optical and electrophysical properties of the structures contained both optically-isotropic and optically-anisotropic materials. One of the ways allowed the information about such materials and structures to be obtained is based on the application of infrared spectroscopy, in particular, specular infrared reflection and attenuated total reflection (ATR) methods. In previous works of the authors [1–12] it was shown that the study of excitation conditions of surface waves (when energy propagates only along the surface or along the interface separated two media [1, 13]) as well as wave propagation through the film-substrate structures permit to extract information on elementary excitations of different types (in particular, phonons and plasmons) and their interaction (phonon-phonon, electron-phonon and electron-electron).

Considerable attention was paid to theoretical and experimental investigation of surface electromagnetic waves in optically isotropic crystals [13, 14] whereas the properties of surface phonon and plasmon-phonon polaritons in optical anisotropic crystals were less addressed [1, 13]. Even less attention was paid to different types of polariton excitations in optically anisotropic semiconductor and dielectric films grown on different substrates. It should be noted that in spite of the fact that optical properties of $Mg_xZn_{1-x}O$ thin films deposited on dielectric (Al_2O_3) and semiconductor (Si, 6H–SiC) substrates were studied [15–26], the polariton excitations were rarely considered [15, 16].

It is known that $Mg_xZn_{1-x}O$ ternary compounds have unique properties: high photosensitivity, high photo- and cathodoluminescence yield, pyro- and piezoelectric effect, etc. Nowadays, the use of the films becomes costly effective in comparison with the production of $Mg_xZn_{1-x}O$ single crystals. Such films are promising for manufacturing a wide variety of new generation optoelectronic devices based on the use of surface and bulk waves [19–26], as well as for anti-reflective, conductive layers in large-area solar cells [16, 27–30], photodetectors etc. Different technological approaches can be used for the deposition of $Mg_xZn_{1-x}O$ films on various substrates such as Si, SiO_2, Al_2O_3, 6H–SiC, etc. The formation of $Mg_xZn_{1-x}O$ solid solution with a bandgap wider than that of ZnO permits to shift the working range of lasers, LEDs and photodetectors towards deeper ultraviolet. This ability to change the optical and electrical properties of ternary $Mg_xZn_{1-x}O$ compounds via Mg content variation extends beyond their application. For the first time this phenomenon was described in the works of Kawasaki et al. [19, 25].

Depending on the Mg and Zn relative concentrations, $Mg_xZn_{1-x}O$ ternary compounds can have both a hexagonal crystal structure (such as wurtzite) and a cubic one. The attractiveness of the study of $Mg_xZn_{1-x}O$ compounds with $x \leq 0.2$ is the preservation of the hexagonal structure and the manifestation of optical-anisotropic properties in the infrared spectral range. For $x > 0.2$, these ternary compounds have a cubic lattice.

Among different possible substrates for the deposition of $Mg_xZn_{1-x}O$ films, a special attention is paid to silicon carbide (SiC). This unique binary compound of silicon and carbon exists in the solid phase and is characterized by a strong ionic-covalent bond, which causes special physicochemical properties (i.e., radiation and chemical resistance) [1, 3, 31, 32]. Single crystals of type 6H–SiC belong to space group C^4_{6V} ($P6_{3mc}$). They are widely used in the development of different devices (fluorescent indicators, nuclear radiation meters, high temperature diodes, high-pressure sensors, etc.) [33]. The 6H–SiC crystals demonstrate also a strong anisotropy of the properties of the plasmon subsystem and a weak anisotropy of the properties of phonon subsystem.

As it is mentioned above, despite of wide possible applications of $Mg_xZn_{1-x}O$ films deposited on optically anisotropic 6H–SiC substrates [16, 27–30], the study of interaction of plasmon and phonon subsystems by polariton spectroscopy method is insufficient. At the same time, such studies make it possible to carry out a comprehensive analysis of the effect of the electrophysical properties of the film and substrate on the characteristics of surface polaritons of the phonon and plasma-phonon type. In the present work, the interaction of the infrared light with optically anisotropic $Mg_xZn_{1-x}O$/6H–SiC structures is investigated in order to obtain information on the conditions for the excitation and propagation of surface phonon and plasmon-phonon polaritons in these structures.

2. Experimental

2.1. Method of polariton spectroscopy for investigation of $Mg_xZn_{1-x}O$/6H–SiC structures

It is known that the method of polariton spectroscopy is one of the non-destructive methods used for the investigation of the optical and electrophysical properties of thin films grown on semiconductor and dielectric substrates. It allows monitoring a film quality and its structural perfection [1, 13, 14], namely, information on physical and chemical properties of the films as well as the parameters of underlying substrate and its surface quality can be extracted.

Surface polariton (SP) is a surface electromagnetic excitation that does not interact itself with excited light during experimental investigation of light absorption and specular reflection because SP dispersion curve does not cross the "light curve". However, this drawback can be overcome by using attenuated total reflection approach as described in [13, 34, 35].

The physical basis of the ATR method is the phenomenon of light penetration from an optically denser medium into an optically less dense one under conditions of total internal reflection. The angle of light incidence must be larger than the critical one.

The surface polaritons are excited in the spectral range of an imaginary wave vector K. To achieve this, a thin airspace (or space filled by other dielectric with a refractive index lower than that of studied sample) has to be formed between the ATR element and the investigated sample. Part of the incident irradiation penetrates into the sample being absorbed in a certain frequency range. As a result, the reflection becomes not total, i.e. being "disturbed" by the total internal reflection. Inside the airspace, an electromagnetic field is formed (the z-axis is directed normally to the crystal surface), being exponentially attenuated along the z-axis. The wave vector K in the airspace has an imaginary value ($K < 0$) that allows the energy and momentum conservation, and hence leads to the absorption of light due to the interaction with surface oscillations.

The ATR method is widely used for the investigation of semiconductor and dielectric films and crystals. The appearance of surface waves affects the ATR spectra. For instance, the minima can appear in the ATR spectra in the range of "residual rays" ("reststrahlen" band) of the material studied at the frequency corresponded to the SP frequency (ν_{SP}). The dependence $\nu_{SP}(K)$ determines the SP dispersion relation that is the main property of surface polaritons.

The possibility of the SP excitation at the interface of two different media is determined by their dielectric constants, $\varepsilon_1(\nu)$ and $\varepsilon_2(\nu)$. A surface electromagnetic wave can propagate along the interface (along the x-axis) only when, at least, one of the media is surface-active, i.e. its dielectric constant in a certain frequency range is negative.

It should be noted that the investigation of surface polaritons at the interface of two surface-active media is a more common. In this case, three relationships are possible between the frequencies of bulk dipole resonances in these media: they do not overlap, partially or fully overlap [1, 13, 14].

2.2. Theory and analysis of ATR spectra of $Mg_xZn_{1-x}O$/6H–SiC structures

There are a number of scientific papers reported on the study of hexagonal single crystals of n-type 6H–SiC by non-destructive methods of IR spectroscopy and surface polaritons [1–7, 33]. Experimental IR reflection spectra from the 6H–SiC surface with a high electron concentration ($n_0 > 10^{18}$ cm^{-3}) were reported at first in [2]. The effect of the anisotropy of the crystal lattice and the effective electron mass, as well as the damping coefficients of phonons γ_f and plasmons γ_p on the surface reflection coefficient $R(\nu)$ of 6H–SiC single crystals in the IR spectral range were studied in [1–7].

The specular IR reflection spectroscopy was earlier used to study the optical characteristics of thin $Mg_xZn_{1-x}O$ films on dielectric Al_2O_3 substrate (i.e. $Mg_xZn_{1-x}O/Al_2O_3$ structures) in [15]. It was shown that the variation of the film thickness and Mg content significantly deform the shape of IR reflection spectrum in the range of "residual rays" of the film and the substrate as well as reduce the reflectivity. Modeling of specular IR reflection spectra allowed determining the static dielectric constant of the $Mg_xZn_{1-x}O$ film at different x values for the orientation of electromagnetic field $E \perp c$ [15]. It is established that the spectra of the $Mg_xZn_{1-x}O/Al_2O_3$ structure are well-modeled by the use of self-consistent parameters for single crystals of MgO, ZnO and "colorless" sapphire (Al_2O_3) with orientation $E \perp c$, which is important for the application of non-destructive IR spectroscopy methods for the determination of optical characteristics of ternary compound films as the degree of their texturing.

In the present work, theoretical investigation of the specular IR reflection spectra of the $Mg_xZn_{1-x}O$ films on semi-infinite semiconductor substrate 6H–SiC were performed in the range of "residual rays" of MgO, ZnO and 6H–SiC using the equations described [2, 3, 15, 36, 37] for orientation $E \perp c$ taking into account the interaction of IR light radiation with phonon and plasmon subsystems of $Mg_xZn_{1-x}O$ film and semi-infinite 6H–SiC substrate. The calculation was performed using the model for dielectric permittivity with additive contribution of active optical phonons and plasmons of the film and substrate [15, 36]:

$$\varepsilon(\nu) = \varepsilon'(\nu) + i\varepsilon''(\nu) = \varepsilon_\infty \cdot \left(1 + \frac{(\nu_L^2 - \nu_T^2)}{\nu_T^2 - \nu^2 - i\nu\gamma_f} - \frac{\nu_p^2}{\nu^2 + i\nu\gamma_p)}\right) \quad (1)$$

where for both the film and the substrate the parameters are: ν_L and ν_T are the frequency of longitudinal and transverse optical phonons, respectively, γ_f is the damping coefficient of optical phonon of the films and substrate; γ_p and ν_p are the damping coefficient and plasmon frequency, respectively. The SP study was performed without consideration of the absorption ability of the film and substrate in IR spectral range.

Figure 1 demonstrates the theoretical real part of dielectric constant $\varepsilon'(\nu)$ of the $Mg_xZn_{1-x}O$ film (curve *1*) and the 6H–SiC substrate (curve *2*). The calculation was made for the spectral range in which the appearance of surface phonons and phonopolaritons at the film/air and film/substrate interfaces is possible (shown by solid bold lines) [1, 13]. It is seen that the range of anomalous dispersion of $Mg_xZn_{1-x}O$ and 6H–SiC appear in different spectral interval. Each medium is surface active, whereas the corresponding frequency range is $\nu = 418–424$, 517–553 and 601–796 cm^{-1} for $Mg_xZn_{1-x}O$ film and $\nu = 810–960$ cm^{-1} for 6H–SiC substrate. The latter one is not surface active.

Applying the ATR method, one can merge the peculiarities of the SP propagation in the optically anisotropic structures such as $Mg_xZn_{1-x}O$/6H–SiC for orientation of the SP wave vector towards the structure surface as $E \perp c$.

Let us consider that the z-axis propagates through the structure being perpendicular to the interface between two media. In this case, the anisotropic medium with dielectric permittivity $\varepsilon_1(\nu)$ occupies the space with $z < 0$ and the isotropic medium with $\varepsilon_2(\nu)$ occupied the space with $z > 0$.

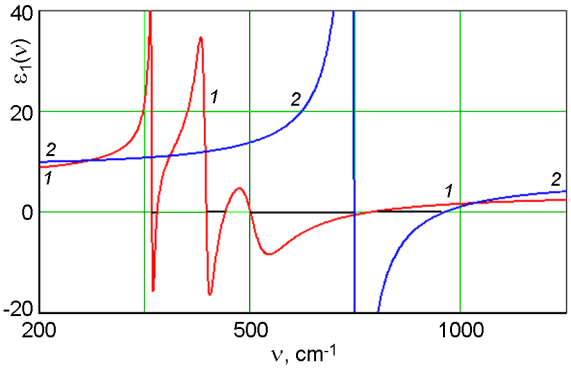

Fig. 1. Frequency dependences of real part of dielectric constant $\varepsilon_1(\nu)$ for orientation $E \perp c$: curve *1* — MgZnO; curve *2* — 6H—SiC.

The electrical field vector E of surface wave propagates in the xy-plane and damps exponentially along the z-axis from media interface towards their bulk.

The calculation of the ATR spectra was carried out using the formula described in [1, 9, 13, 36] and considering also the interaction of IR irradiation with phonon and plasmon subsystems of $Mg_xZn_{1-x}O$ film and semi-infinite 6H–SiC substrate for orientation $E \perp c$:

$$R(\nu,\varphi) = \left[\frac{1 + iP(\nu,\varphi)}{1 - iP(\nu,\varphi)}\right]^2, \quad (2)$$

where

$$P(\nu,\varphi) := \frac{\beta_2(\nu,\varphi)}{\beta_1(\nu,\varphi)} \cdot \frac{\beta_3(\nu,\varphi) \cdot A(\nu,\varphi) + \beta_2(\nu,\varphi) \cdot \tanh(2\pi\nu \cdot d_f \cdot k_2(\nu,\varphi))}{\beta_2(\nu,\varphi) \cdot A(\nu,\varphi) + \beta_3(\nu,\varphi) \cdot \tanh(2\pi\nu \cdot d_f \cdot k_2(\nu,\varphi))}$$

$$A(\nu,\varphi) = \frac{\beta_4(\nu,\varphi)}{\beta_3(\nu,\varphi)} \cdot \frac{\beta_3(\nu,\varphi) \cdot \tanh(2\pi\nu \cdot d_f \cdot k_3(\nu,\varphi))}{\beta_4(\nu,\varphi) \cdot \tanh(2\pi\nu \cdot d_f \cdot k_3(\nu,\varphi))}$$

$$\beta_1(\nu,\varphi) = \frac{\varepsilon_1}{k_1(\nu,\varphi)};\ k_1(\nu,\varphi) = \sqrt{\varepsilon_1} \cdot \cos(\varphi);$$

$$\beta_2(\nu,\varphi) = \frac{\varepsilon_2}{k_2(\nu,\varphi)};\quad k_2(\nu,\varphi) = \sqrt{(k_x(\nu,\varphi))^2 - \varepsilon_2}$$

$$\beta_3(\nu,\varphi) = \frac{\varepsilon_3(\nu,\varphi)}{k_3(\nu,\varphi)};\ k_3(\nu,\varphi) = \sqrt{(k_x(\nu,\varphi))^2 - \varepsilon_3(\nu,\varphi)}$$

$$\beta_4(\nu,\varphi) = \frac{\varepsilon_4(\nu,\varphi)}{k_4(\nu,\varphi)};\ k_4(\nu,\varphi) = \sqrt{(k_x(\nu,\varphi))^2 - \varepsilon_4(\nu,\varphi)}$$

$$k_x(\nu,\varphi) = \sqrt{\varepsilon_1} \cdot \sin(\varphi)$$

k_x is the component of wave-vector K along x-axis $k_y = k_z = 0$ and the indexes 1–4 correspond to the ATR prism, airspace with thickness d_c, semiconductor film $Mg_xZn_{1-x}O$ with the thickness d_f and semi-infinite semiconductor substrate 6H–SiC, respectively.

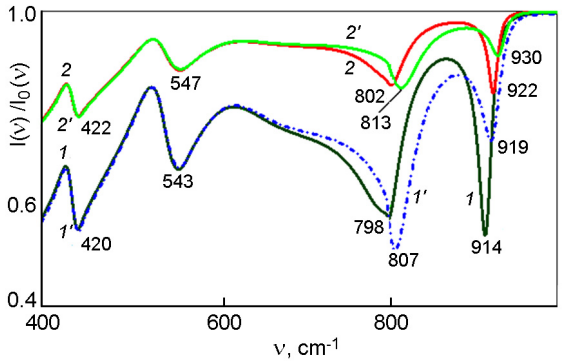

Fig. 2. ATR spectra of $Mg_{0.2}Zn_{0.8}O$/6H–SiC structure: curves *1*, *2* — undoped $Mg_{0.2}Zn_{0.8}O$ film on undoped 6H–SiC substrate; curves *1′*, *2′* — undoped film $Mg_{0.2}Zn_{0.8}O$ on doped substrate 6H–SiC; φ = 30° (curves *1* and *1′*) and φ = 33° (curves *2* and *2′*); orientation $E \perp c$ for all curves.

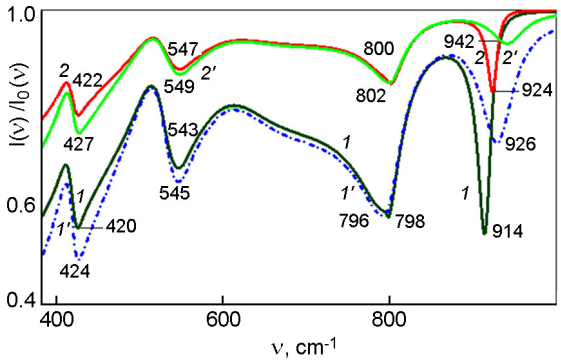

Fig. 3. ATR spectra of $Mg_{0.2}Zn_{0.8}O$/6H–SiC structure: curves *1*, *2* — undoped $Mg_{0.2}Zn_{0.8}O$ film on undoped 6H–SiC substrate; curves *1′*, *2′* — doped film $Mg_{0.2}Zn_{0.8}O$ on undoped substrate 6H–SiC; φ = 30° (curves *1* and *1′*) and φ = 33° (curves *2* and *2′*); orientation $E \perp c$ for all curves.

3. Results and discussion

The $R(\nu,\varphi) = \dfrac{I(\nu,\varphi)}{I_0(\nu,\varphi)}$, where $I(\nu,\varphi)$, $I_0(\nu,\varphi)$ are the reflective and incident intensities of the IR light. The $\varepsilon_3(\nu)$ and $\varepsilon_4(\nu)$ are the dielectric constants of the film and substrate, respectively, that additively considered the contribution of optically active transverse phonons ν_T and plasmons ν_p, i.e.

$$\varepsilon_{3,4}(\nu) = \varepsilon_{\infty_{3,4}}\left(1 + \frac{\nu_{T_{3,4}}(\varepsilon_{0_{3,4}} - \varepsilon_{\infty_{3,4}})}{\nu_{T_{3,4}}^2 - \nu^2 - i\nu\gamma_{f_{3,4}}} - \frac{\nu_{p_{3,4}}^2}{\nu^2 + i\nu\gamma_{p_{3,4}}}\right).$$

All other notations are commonly used.

Figures 2 and 3 show the ATR spectra in the 350–1000 cm^{-1} range for $Mg_{0.2}Zn_{0.8}O$/6H–SiC structure for $E \perp c$ (curves *1*, *2*) calculated for the angle of incident IR light in ATR prism φ = 30° (curves *1* and *1′*) and φ = 33° (curves *2* and *2′*) under constant airspace between the prism and the sample. The calculation was performed using the approach described in [38] and the parameters of phonon subsystems of the $Mg_{0.2}Zn_{0.8}O$ film and 6H–SiC substrate given in Table. It was also considered that the plasmon subsystem does not affect the ATR spectra.

As one can see from Fig. 2, the comparison of curves 1 and 1′ shows that the increase of the free carrier concentration (electrons) in 6H–SiC substrate up to $n_0 = 5 \cdot 10^{18}$ cm^{-3} (that corresponds to the damping coefficient of transverse optical phonon $\gamma_{f\perp 4} = 20$ cm^{-1}, and frequency and damping coefficient of plasmons $\nu_{p\perp 4} = 550$ cm^{-1} and $\gamma_{p\perp 4} = 620$ cm^{-1}, respectively) results in the difference of the ATR spectra in the 700–1000 cm^{-1} spectral range which characterizes the range of residual rays of the 6H–SiC substrate for $E \perp c$. The increase of the n_0 value in the $Mg_{0.2}Zn_{0.8}O$ film ($\nu_{p\perp 3} = 550$ cm^{-1}, $\gamma_{p\perp 3} = 620$ cm^{-1}) results in the appearance of the difference between the spectra in whole spectral range (Fig. 3), and, more significant, in the 380–600 and 800–1000 cm^{-1} spectral ranges (curves *1*, *1′*).

The sharp variation of the reflection coefficient $R(\nu)$ occurs in the 400–600 and 700–1000 cm^{-1} intervals. The curves *1* and *2* in Fig. 2 and 3 are the same. They are shown to make easy the comparison of the ATR spectra for the structures with different carrier concentration (undoped and doped). The calculation for undoped structure was performed for $d_f = 0.5$ μm and with $\nu_{p\perp 3,4} = \gamma_{p\perp 3,4} = 1$ cm^{-1}, $\gamma_{f\perp 4} = 3$ cm^{-1} (indexes 1 and 2 correspond to the film and substrate, respectively). The comparison of

Table. Parameters of phonon subsystems of $Mg_{0.2}Zn_{0.8}O$ film and 6H–SiC materials

Parameter	ε_∞	ε_0	ν_{T_1}, cm^{-1}	ΔS_1	γ_{f_1}, cm^{-1}	ν_{T_2}, cm^{-1}	ΔS_2	γ_{f_2}, cm^{-1}	ν_{T_f}, cm^{-1}	ΔS_2	γ_{f_3}, cm^{-1}
$Mg_{0.2}Zn_{0.8}O$	3.51	8.0	414.1	0.69	13.8	551.8	1.8	17.7	605	2.0	70.7

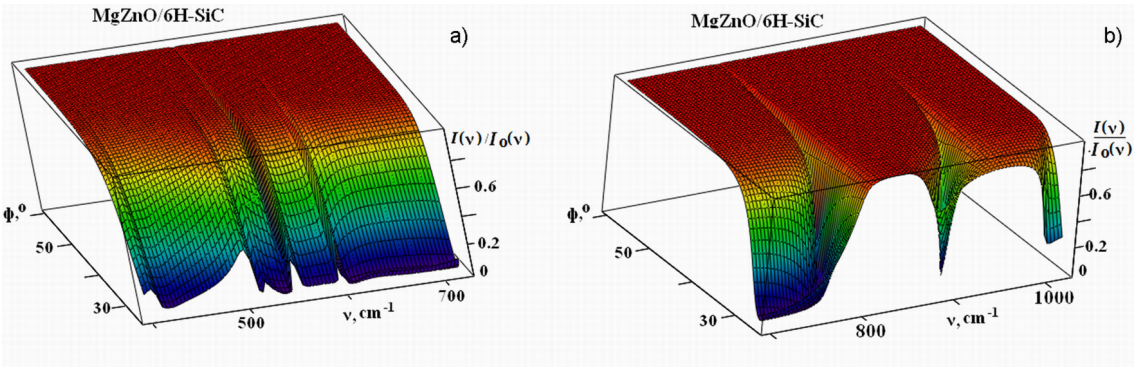

Fig. 4. The surface of modified ATR spectra of $Mg_xZn_{1-x}O$ film on optically anisotropic 6H–SiC substrate for orientation $E \perp c$ obtained for the 400–700 cm^{-1} spectral range (a) and for the 700–1000 cm^{-1} range (b).

the curves *1* and *1′* and curves *2* and *2′* demonstrated by the Fig. 2 and 3 allowed the spectral range of the effect of plasmon subsystem of the substrate (Fig. 2) and the film (Fig. 3) on ATR spectra of $Mg_{0.2}Zn_{0.8}O$/6H–SiC structure to be revealed. In fact, the difference in the ATR spectra between the "highly doped film — undoped substrate" structure (Fig. 2) and "undoped film — highly doped substrates" one (Fig. 3) is clearly seen.

One can point out that calculated ATR spectra demonstrate the same peculiarities that were earlier observed by us in ZnO, MgO and 6H–SiC single crystals, namely: the decrease of the intensity and significant broadening of SP spectrum in the range of residual rays with the increase of the angle of IR light incidence (ATR prism angle), an appearance of asymmetry of ATR maximum and shift of its peak position towards low-frequency range (see, for instance, [1, 5, 6, 37]).

The analysis of the ATR spectra shows the existence of the surface polaritons of "non-radiative" type in the system "vacuum (air) — $Mg_xZn_{1-x}O$ film — 6H–SiC substrate" that propagate along the *x*-axis and damp along the *z*-axis in both directions from the interface "vacuum (air) — film" and "film — substrate". The mentioned electro-magnetic vibrations are polarized in the *xz*-plane.

The appearance of several minima in ATR spectra only under *p*-polarized IR excitation and the negative values of the dielectric constant (in the range between transverse optical and longitudinal phonons) are the evidences of the possibility of the existence of surface polaritons in the $Mg_xZn_{1-x}O$/6H–SiC structure. Besides, the ATR minima shift towards high-frequency range under the increase of ATR prism angle and decrease of light absorption under the constant airspace between the ATR prism and surface of $Mg_xZn_{1-x}O$/6H–SiC sample [1, 13].

As one can see from Fig. 2 and 3, there are minima in ATR spectra corresponded to the surface polaritons of $Mg_{0.2}Zn_{0.8}O$ film and 6H–SiC substrate. Along with this, the increase of carrier concentration manifests itself in the shift and broadening of ATR minima.

It is worth to point out that in the $Mg_xZn_{1-x}O$/6H–SiC structures, the substrate has significant anisotropy of plasmon subsystem contrary to the film [2] and, consequently, in ATR spectra of such structures it is possible the existence of two SPs at the "film/vacuum(air)" interface as well as three SPs at the "film/substrate" interface. The ATR spectra in Figs. 2 and 3 are obtained versus the frequency for fixed ATR prism angle. However, in the [1, 13] it was shown the possibility for calculation of ATR spectra versus prism angle at fixed frequency of IR light. Each of these approaches has advantages and drawbacks. The most complete information can be obtained for the family of ATR spectra (i.e. ATR surface) when all possible prism angles and whole frequency range of IR excitation light are considered. In our case, the calculation was performed for $\nu = 200–1500$ cm^{-1}, $\varphi = 25–60°$, and ATR prism made from KRS-5 material with refractive index 2.38.

The ATR surface shows the 3D-presentation of transmission coefficient of $Mg_{0.2}Zn_{0.8}O$/6H–SiC structure as a function of scanned frequency and prism angle. When there is no interaction of excited light with the structure, this ATR surface is flat ($I(\nu)/I_0(\nu) = 1$). In opposite case, a number of valleys appears (Fig. 4). The deepness of these valleys depends on the airspace between the ATR prism and the sample surface as well as on the frequency and prism angle.

The frequency of the minimum of the ATR surface corresponds to the SP frequency. The evidence of the existence of SP excitations in the structure is the fact that ATR minimum shifts towards higher frequencies and narrows when prism angle increases (Fig. 4).

Figure 4 shows the ATR surface of lightly doped $Mg_{0.2}Zn_{0.8}O$/6H–SiC structure in the spectral ranges of 400–600 cm^{-1} (Fig. 4,a) and 800–1000 cm^{-1} (Fig. 4,b) taken for φ = 25–60°, d_f = 0.5 μm and d_c = 5 μm.

It is worth to point out that the variation of d_f from 0,001 up to 0.05 μm did not affect ATR spectra. However, further d_f increase under constant other parameters of phonon and plasmon subsystems of the $Mg_xZn_{1-x}O$ film results in significant transformation of ATR spectra in the range of residual rays of the film and substrate. For $d_f > 0{,}1$ μm the ATR minima become to be closer in the range of SP existence for $Mg_xZn_{1-x}O$ film. The calculation showed also the coincidence of the high and low frequency minima in ATR spectra for the film with d_f = 10 μm that is in good agreement with the data obtained for $Mg_xZn_{1-x}O$ single crystal. In the ATR spectra only one minimum exists in the 300–800 cm^{-1} spectral range whatever the φ value.

Figure 4,b demonstrates the ATR spectra in the 700–1000 cm^{-1} spectral range that corresponds to the range of residual rays of the 6H–SiC substrate. It is seen that the decreasing of the φ from 40 down to 25° shifts the minimum from 956 up to 960 cm^{-1}. Taking into account the damping of optical phonons, the appearance of an additional valley at the $I(\nu)/I_0(\nu)$ surface can be predicted and experimentally detected under the variation of the φ value.

Figure 5 shows the dispersion relation for the $Mg_{0.2}Zn_{0.8}O$/6H–SiC structure for orientation $E \perp c$. The calculation of dispersion branches of surface polaritons was performed using the formula for SP dispersion in three-layer structure as "vacuum — film — substrate" [9, 34, 38, 39] and data of Table:

$$(\beta_1 + \beta_2)(\beta_2 + \beta_3) + (\beta_1 - \beta_2)(\beta_2 - \beta_3)\exp(-2\chi_2 d) = 0, \quad (3)$$

where $\beta_j = \varepsilon_j/\chi_j$, $\chi_j = [K^2 - \varepsilon_j(\nu)\omega^2/c^2]^{1/2}$, $\omega = 2\pi\nu$, j = 1, 2, 3; (1 — vacuum (air); 2 — $Mg_{0.2}Zn_{0.8}O$ film; 3 — 6H–SiC substrate); $\varepsilon_{2,3} = \varepsilon_{\infty 2,3} + \dfrac{\omega^2_{T_{2,3}}(\varepsilon_{o_{2,3}} - \varepsilon_{\infty_{2,3}})}{\omega^2_{T_{2,3}} - \omega^2 - i\omega\gamma_{f_{2,3}}}$; ε_1 = 1, ω_T is the angular frequency of optical transverse phonon; K is the SP wave vector.

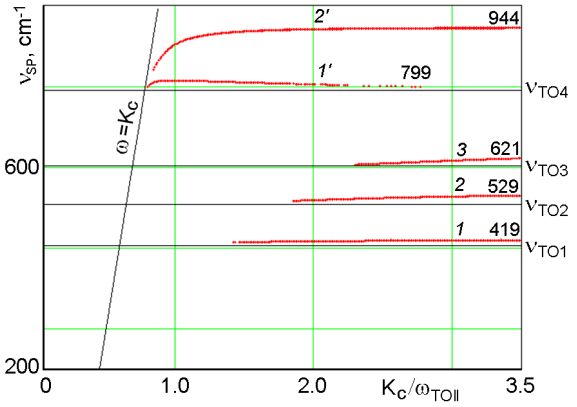

Fig. 5. Dispersion relations of phonon surface polaritons for $Mg_xZn_{1-x}O$/6H–SiC structure for orientation $E \perp c$. The parameters of the $Mg_{0.2}Zn_{0.8}O$ film are d_f = 0.5 μm, ν_{p_3} = 1 cm^{-1}, γ_{p_3} = 1 cm^{-1} and parameters of the 6H–SiC substrate are ν_{p_4} = 1 cm^{-1}, γ_{p_4} = 1 cm^{-1} and γ_{f_4} = 3 cm^{-1}. The airspace between the ATR prism and the structure surface is d_c = 5 μm.

The theoretical dependences $\nu_{SP} = f(Kc/\omega_{TO})$ (here, c is light velosity) obtained for the $Mg_{0.2}Zn_{0.8}O$ film are shown by the curves *1–3* and for the 6H–SiC substrate — by the curves *1′* and *2′* (Fig. 5) for orientation $E \perp c$ and d_f = 0.5 μm. The cut-off frequencies of surface polaritons for the films were found at 419, 529 and 621 cm^{-1} (curves *1–3*) and for the substrate at 799 and 944 cm^{-1} (curves *1′* and *2′*) for the Kc/ω_{TO}= 3.5. It was also observed that the decrease of the film thickness results in the decreasing of effect of the $Mg_{0.2}Zn_{0.8}O$ film on the dispersion relation of the 6H–SiC substrate for the orientation $E \perp c$ and for d_f < 0.05 μm this effect is negligible.

4. Conclusions

In this work it was shown that the surface polaritons in semiconductor $Mg_xZn_{1-x}O$/6H–SiC structures can be predicted using the model with additive oscillator contribution and self-consisted parameters determined for the MgO, ZnO and 6H–SiC single crystals for orientation $E \perp c$. It was demonstrated that in $Mg_xZn_{1-x}O$/6H–SiC structures the excitation and propagation of surface polaritons of phonon and phonon-plasmon types are possible. The numerical simulation of dispersion relations was performed for the

$Mg_xZn_{1-x}O$/6H–SiC structure using experimentally determined oscillator parameters. The dispersion dependences for such structure were obtained for the first time. The spectral ranges of the existence of surface polaritons in the ATR spectra registered as a function of the angle of the IR excitation incidence at fixed light frequency and vice versa were obtained. The application of infrared spectroscopy as a non-destructive method for the characterization of the films of ternary compounds was demonstrated.

Acknowledgements. This work was supported by the National Research Foundation of Ukraine from the state budget, project 2020.02/0380 "Structure transformation and non-equilibrium electron processes in wide bandgap metal oxides and their solid solutions".

References

1. E.F.Venger, A.V.Melnichuk, Yu.A.Pasechnik, Spectroscopy of Residual Rays, Naukova Dumka, Kiev (2001).
2. A.V.Melnichuk, Yu.A.Pasechnik, *Fiz. Tv. Tela*, **34**, 423 (1992).
3. E.F.Venger, A.V Melnichuk, L.Yu.Melnichuk, Yu.A.Pasechnik, *Phys. Stat. Sol. B*, **188**, 823 (1995). doi.org/10.1002/pssb.2221880226.
4. O.Melnichuk, L.Melnichuk, B.Tsykaniuk et al., *Thin Solid Films*, **673**, 136 (2019). doi:10.1016/j.tsf.2019.01.028.
5. A.V.Melnichuk, *J. Surf. Invest.. X-Ray, Synchrotron Neutron Techn.*, **7**, 76 (1998).
6. E.F.Venger, L.Yu.Melnichuk, A.V.Melnichuk et al., *Ukr. Fiz. Zh.*, **43**, 598 (1998).
7. A.V.Melnichuk, Yu.A.Pasechnik, *Phys. Solid State*, **40**, 582 (1998). https://doi.org/10.1134/1.1130355].
8. E.F.Venger, A.I.Ievtushenko, L.Yu.Melnichuk, O.V.Melnichuk, *Phys. Chem. Solid States*, **12**, 579 (2011).
9. N.Korsunska, L.Borkovska, Yu.Polischuk et al., *Mater. Sci. Semicond. Process.*, **94**, 51 (2019).
10. E.F.Venger, A.I.Ievtushenko, L.Yu.Melnichuk, O.V.Melnichuk, *Semicond. Phys., Quantum Electron. Optoelectron.*, **13**, 314 (2010).
11. I.Markevich, L.Borkovska, Y.Venger et al., *Ukr. Fiz. Zh. Oglyady*, **13**, 57 (2018) [in Ukrainian]. https://ujp.bitp.kiev.ua/index.php/ujp/article/view/2018235
12. O.V.Melnichuk, L.Yu.Melnichuk, N.O.Korsunska et al., *Ukr. Fiz. Zh.*, **64**, 434 (2019). doi.org/10.15407/ujpe64.5.434 [in English].
13. N.L.Dmitruk, V.G.Litovchenko, V.L.Strizhevsky, Surface Polaritons in Semiconductors and Dielectrics, Naukova Dumka, Kyiv (1989).
14. E.A.Vinogradov, N.N.Novikova, V.A.Yakovlev, *Phys.Uspekhi*, **184**, 653 (2014).
15. E.F.Venger, I.V.Venger, N.O.Korsunska et al., *Semicond. Phys., Quantum Electron. Optoelectron.*, **21**, 417 (2018).
16. Ye.F.Venger, I.V.Venger, D.V.Korbutyak et al., Mater. Intern. Conf. "Functional Materials for Innovative Energy", FMIE-2019", Kyiv (2019), p.4 (Y24).
17. D.Thapa, J.Huso, J.Lapp et al., *J. Mater. Sci.:Mater. Electron.*, **29**, 16782 (2018).
18. L.Borkovska, L.Khomenkova, I.Markevich et al., *Phys. Stat. Sol. A*, **215**, 1800250 (2018).
19. A.Ohtomo, M.Kawasaki, T.Koida et al., *Appl. Phys. Lett.*, **71**, 2466 (1998).
20. A.Ohtomo, K.Tamura, M.Kawasaki et al., *Appl. Phys. Lett.*, **77**, 2204 (2000). doi.org/10.1063/1.1315340.
21. Y.Jin, B.Zhang, Y.Shuming et al., *Solid State Commun.*, **119**, 409 (2001).
22. A.Kaushal, D.Kaur, *Solar Energy Mater. Solar Cells*, **93**, 193 (2009).
23. J.Chen, W.Z.Shen, *Appl. Phys. Lett.*, **83**, 2154 (2003). doi.org/10.1063/1.1610795.
24. C.Bundesmann, A.Rahm, M.Lorenz, M.Grundmann, *J. Appl. Phys.*, **99**, 113504 (2006).
25. T.Makino, Y.Segawa, A.Ohtomo et al., *Appl. Phys. Lett.*, **78**, 1237 (2001).
26. Th.Gruber, C.Kirchner, R.Kling et al., *Appl. Phys. Lett.*, **84**, 5359 (2004).
27. U.Rau, D.Abou-Ras, T.Kirchartz, WILEY-VCH Verlag GmbH & Co. KGaA, 139 (2011).
28. N.A.Kovtun, B.T.Boyko, G.S.Khripunov, V.R.Kopach, *Probl. Atom. Sci. Techn.*, **10**, 75 (1999).
29. N.V.Romanova, General and Inorganic Chemistry, VTF "Perun" (1998).
30. P.I.Baransky, V.P.Klochkov, I.V.Potikevich. Semiconductor Electronics. Properties of Materials: Reference Book, Naukova Dumka, Kyiv (1975),
31. P.A.Ivanov, V.E.Shuttles, *Semicond. Phys. Techn. J.*, **29**, 1921 (1995).
32. I.N.Frantsevich, G.G.Gnesin, S.M.Zubkova et al., Silicon Carbide, Properties and Applications, Naukova Dumka, Kyiv (1975).
33. O.A.Ageev, A.E.Belyaev, N.S.Boltovets et al., Silicon Carbide: Technology, Properties, Application, ISMA, Kharkov (2010).
34. G.I.Dovbeshko, A.V.Melnichuk, S.V.Ogurtsov et al., *Ukr. Fiz. Zh.*, **42**, 728 (1997).
35. G.I.Dovbesko, S.V.Ogurtsov, G.A.Pushkovskaya et al., *Mol. Struct.*, **114**, 305 (1984). doi.org/10.1016/0022-2860(84)87150-1.
36. E.F.Venger, L.Yu.Melnichuk, A.V.Melnichuk, T.V.Semikina, *Ukr. Fiz. Zh.*, **61**, 1059 (2016). doi.org/10.15407/ujpe61.12.1053
37. E.F.Venger, A.I.Yevtushenko, D.V.Korbutyak et al., *Phys. Mathem. Notes: Collection Sci. Works*, **53** (2010).
38. E.F.Venger, S.M.Davidenko, L.Yu.Melnichuk et al., *Optoelectr. Semicond. Engin.*, **35**, 190 (2000).
39. A.V.Melnichuk, *Ukr. Fiz. Zh.*, **43**, 1310 (1998).